

# Comparison of the Adsorption of Linear Alkanesulfonate and Linear Alkylbenzenesulfonate Surfactants at Liquid Interfaces

M. R. Watry and G. L. Richmond\*

Department of Chemistry, University of Oregon, Eugene, Oregon 97403

Received May 27, 1999

**Abstract:** Linear alkanesulfonates and linear alkylbenzenesulfonates constitute a large fraction of the surfactants used in commercial detergents and cleansers. Despite the industrial significance and the possible environmental impact of these compounds, very little is known regarding the molecular properties of these compounds and how they relate to macroscopic properties desired in applications. This study employs vibrational sum frequency spectroscopy (VSFS) to examine and compare the molecular structure of surfactants in these two classes as they adsorb at organic/water and air/water interfaces. The linear alkane- and alkylbenzenesulfonates studied are, respectively, dodecanesulfonate and dodecylbenzenesulfonate. By measurement and comparison of the vibrational spectra of these adsorbed surfactants, changes in the orientation of the aromatic ring and the conformation of the alkyl chains are examined as a function of the number density of surfactant molecules at the interface. The change in aromatic ring orientation as a function of surface concentration is quite different for the dodecylbenzenesulfonate at the air/water interface relative to that at the organic/water interface (CCl<sub>4</sub>/water). The alkyl chains of the dodecylbenzenesulfonate are highly disordered at both interfaces as a function of interfacial concentration, in stark contrast to what is observed for the dodecanesulfonate. These results are discussed in terms of the disruptive nature of the benzene ring and the higher degree of hydrophobicity of the alkyl chain relative to the benzene ring near the ionic sulfonate group.

## 1. Introduction

Manufactured surfactants are ubiquitous in industry and in the home. They are used in almost every household cleaning product, in virtually every personal care product, and in the manufacturing processes of every industry.<sup>1,2</sup> In 1997, two major markets (household and industrial and institutional cleaning products) consumed more than 60% of the 5.14 billion pounds of surfactants produced in the U.S. A common group of industrial and commercial surfactants are the linear alkylbenzenesulfonates (LABS).<sup>3,4</sup> LABS are the predominant surfactant in commercial detergent preparations,<sup>1</sup> and they are often used in specialty cleansers.<sup>2</sup> With such widespread use, these compounds are a serious concern in wastewater treatment and surface water pollution.<sup>5</sup> Economically it is desirable to create new surfactants that are both excellent emulsifiers and easily degradable in the wastewater treatment process and in the environment. To understand which molecular properties of the alkylbenzenesulfonates are responsible for both its efficacy and any possible environmental effects, further investigations are warranted.

Current data available describing alkylbenzenesulfonates at interfaces are largely thermodynamic, elucidating only the macroscopic properties of these systems. Ideally one would like to directly measure the interactions between surfactant molecules

in the micelle because detergents work by solubilizing dirt and oil in micelles in aqueous solution. However, this is extremely difficult. Surfactants adsorbed at a planar surface such as an air/liquid or a liquid/liquid interface offer a more accessible means of studying these interactions, and the experiments described herein are intended to provide information of this nature. The orientation and conformation of an alkylbenzenesulfonate adsorbed at liquid interfaces are examined using the surface specific technique of sum frequency generation. This study describes the first measurements of the vibrational spectra of a LABS at liquid interfaces. The results are compared with similar studies of a related alkanesulfonate.

Since the number of soluble surfactant molecules adsorbed to an interface is orders of magnitude less than the number in bulk solution, molecular level investigations of the interfacial region have been nearly impossible due to the overwhelming response from the bulk. Only a few techniques are available which can distinguish molecules at the interface from those in the bulk. Nonlinear optical techniques such as sum-frequency generation and second harmonic generation are useful techniques for the study of interfaces because these processes are forbidden in centrosymmetric media (under the dipole approximation).<sup>6–8</sup> In these studies we have utilized the surface specificity of vibrational sum-frequency spectroscopy (VSFS) to probe the conformations of surfactant molecules at an interface. Through judicious choices of the polarizations of the light incident on the surface and the analyzed light, and from the intensities of select bands in the vibrational spectra, we are able to determine

(1) Fellows, R.; Heywood, F. W. *The Structure, Performance and Environmental Aspects of Linear Alkylbenzene Sulphonate*; Fellows, R., Heywood, F. W., Eds.; The Royal Society of Chemistry: Cambridge, U.K., 1992; pp 63–81.

(2) Morse, P. M. *Chem. Eng. News* **1999**, 77 (5), 35–48.

(3) Porter, M. R. *Handbook of Surfactants*, 2nd ed.; Chapman and Hall: Glasgow, U.K., 1994.

(4) Karsa, D. R. *Industrial Applications of Surfactants-An Overview*; Karsa, D. R., Ed.; The Royal Society of London: London, 1987; pp 1–23.

(5) Nielson, A. M.; Britton, L. N.; Beall, C. E.; McCormick, T. P.; Russel, G. L. *Environ. Sci. Technol.* **1997**, 31, 3397–3404.

(6) Shen, Y. R. *The Principles of Nonlinear Optics*; Wiley: New York, 1984.

(7) Duffy, D. C.; Davies, P. B.; Bain, C. D. *J. Phys. Chem.* **1995**, 99, 15241–15246.

(8) Eisenthal, K. B. *Chem. Rev.* **1996**, 96, 1343–1360.

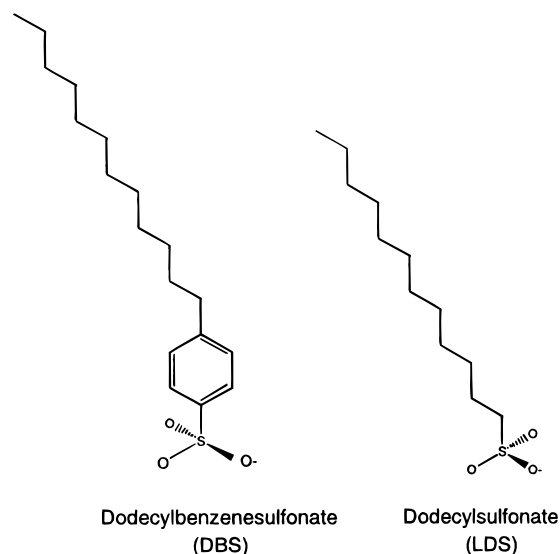


**Figure 1.** Molecular structure of linear dodecanesulfonate (LDS) and linear dodecylbenzenesulfonate (DBS). The sodium salts were used in the experiments described in the text.

the relative conformations of molecules at an interface as a function of surface concentration.<sup>9,10</sup> Since we are analyzing vibrational modes, we can investigate the conformational changes in specific parts of the molecules, and these conformational changes give an insight into the interactions between the surfactant molecules at the interface. In this study the focus is on linear *p*-dodecylbenzenesulfonate sodium salt (DBS) at the air/water and the CCl<sub>4</sub>/water interfaces. Comparisons are made between these systems and similar ones of linear alkanesulfonates to elucidate the effect of the aromatic substituent on the absorptive properties of DBS. The molecular structures of DBS and linear dodecanesulfonate (LDS) are shown in Figure 1.

## 2. Background

**A. Surface Tension.** Surface pressure measurements and VSFS provide complementary information about the concentration-dependent ordering and structure of surfactants at interfaces. To quantify spectral data, it is necessary to determine the number of molecules present at the interface. Analyses of surface pressure data provide the number density of surface-active molecules at the interface.<sup>11</sup> Surface pressure measurements yield isotherms of surface pressure as a function of bulk solution concentration, and these isotherms provide the limiting (maximum) concentration of molecules at the interface through use of the Gibbs equation:<sup>12</sup>

$$\Gamma_i = \frac{1}{nRT} \left( \frac{\partial \pi}{\partial \ln(a_i)} \right)_T \quad (1)$$

Here  $\Gamma_i$  is the surface excess concentration at maximum surface coverage,  $\pi$  is the interfacial pressure in mN/m,  $n$  is the number of species in excess at the interface, and  $a_i$  is the activity. In the studies described below,  $n = 1$  for solutions with excess

salt and  $n = 2$  for solutions without excess salt.<sup>13</sup> (Although there has been some recent discussion as to whether these values are always correct,<sup>14</sup> we believe that they provide the most accurate representation of these data.) For dilute solutions (less than 10<sup>-2</sup> M), the activity can be replaced with the bulk concentration  $C_i$ . The surface coverages for less concentrated solutions are obtained by inserting the maximum surface concentration and the measured surface pressure into the Frumkin equation:<sup>11</sup>

$$\pi_2 = -\Gamma_i \ln \left[ 1 - \frac{\Gamma_2}{\Gamma_i} \right] \quad (2)$$

Here the subscript 2 refers to quantities for any specific bulk concentration.

**B. Spectroscopy.** VSFS takes advantage of the break in inversion symmetry occurring at an interface to generate nonlinear optical fields through the molecular hyperpolarizability.<sup>15,16</sup> The intensity of the sum-frequency (SF) signal depends on the Fresnel coefficients for each of the fields,  $f_{\text{SF}}$ ,  $f_{\text{vis}}$ , and  $f_{\text{IR}}$ , and the second-order susceptibility of the molecules at the interface,  $\chi^{(2)}$ , in the following way:

$$I(\omega_{\text{SF}}) = |\tilde{f}_{\text{SF}} f_{\text{vis}} f_{\text{IR}} \chi^{(2)}|^2 I_{\text{vis}} I_{\text{IR}} \quad (3)$$

The second-order susceptibility can be written as the sum of a nonresonant term and a resonant term:

$$\chi^{(2)} = \chi_{\text{NR}}^{(2)} + \sum_{\nu} \chi_{\text{R}}^{(2)}(\nu) \quad (4)$$

Here the resonant term is summed over all vibrational resonances of the molecules at the interface. The nonresonant term is negligible in our experiments. For an IR vibrational mode, the resonant component of the susceptibility is given by

$$(\chi_{\text{R}}^{(2)}(\omega_{\nu}))_{lmn} = \frac{NA_{n_{\nu}} M_{lm_{\nu}}}{(\omega_{\nu} - \omega_{\text{IR}} - i\Gamma_{\nu})} \quad (5)$$

where  $N$  is the adsorbate surface number density,  $A_{n_{\nu}}$  is the IR transition moment,  $M_{lm_{\nu}}$  is the Raman transition strength,  $\omega_{\nu}$  is the transition frequency with damping constant  $\Gamma_{\nu}$  for a specific transition  $\nu$ , and  $\omega_{\text{IR}}$  is the frequency of the incident IR beam. Equation 5 shows that, for a transition to be SF active, it must be both IR and Raman active. Under the dipole approximation, this situation only arises in media lacking inversion symmetry.<sup>6,15-17</sup> (It is important to note that an interface that is isotropic in its plane can still exhibit SF activity as long as there is the absence of inversion symmetry in three dimensions.)

## 3. Experimental Section

**A. Solution Preparation.** NaDBS and NaLDS were purchased from TCI America and used as received. Analytical reagent grade NaCl was purchased from Mallinckrodt and heat dried. HPLC grade water was also purchased from Mallinckrodt and used as received. The 99.9% D<sub>2</sub>O was purchased from Cambridge Isotopes, and 99.9+% HPLC grade CCl<sub>4</sub> was purchased from Sigma and used as received. Aqueous solutions for the DBS studies were prepared by dilution of stock

(9) Guyot-Sionnest, P.; Hunt, J. H.; Shen, Y. R. *Phys. Rev. Lett.* **1987**, *59*, 1597-1600.

(10) Messmer, M. C.; Conboy, J. C.; Richmond, G. L. *J. Am. Chem. Soc.* **1995**, *117*, 8039-8040.

(11) Rosen, M. J. *Surfactants and Interfacial Phenomena*; Wiley-Interscience: New York, 1978.

(12) Gibbs, J. W. *The Collected Works of J. Willard Gibbs*, 2nd ed.; Yale University Press: New Haven, CT, 1948; Vol. 1.

(13) Tajima, K. *Bull. Chem. Soc. Jpn.* **1971**, *44*, 1767-1771.

(14) Bae, S.; Haage, K.; Wantke, K.; Motschmann, H. *J. Phys. Chem. B* **1999**, *103*, 1045-1050.

(15) Dick, B. *Chem. Phys.* **1985**, *96*, 199-215.

(16) Dick, B.; Gierulski, A.; Marowsky, G. *Appl. Phys. B* **1985**, *38*, 107-116.

(17) Chemla, D. S.; Zyss, J. *Nonlinear Optical Properties of Organic Molecules and Crystals*; Academic Press: Orlando, FL, 1987; Vol. 1.

solutions. Aqueous solutions for the LDS studies were prepared individually from the solid. HPLC water was used for all aqueous solutions prepared for surface tension experiments. D<sub>2</sub>O was used for all aqueous solutions prepared for spectroscopic experiments.

**B. Surface Tension.** All surface tension measurements were made using the Wilhelmy plate method.<sup>18,19</sup> A platinum plate cleaned with a mixture of nitric and sulfuric acid, rinsed in HPLC water, and then flamed until glowing was used for the oil/water measurements. This cleaning procedure was repeated before each measurement. A glass microscope cover slip made hydrophilic by soaking overnight in piranha solution, rinsed in HPLC water, and dried was used for the air/water measurements. (*Caution! Piranha solutions are highly oxidizing and should be used with extreme care and in the absence of organic solvents and materials.*) The plate was rinsed and dried between measurements.

For the CCl<sub>4</sub>/water measurements, 20 mL of CCl<sub>4</sub> was pipetted into a crystallization dish 60 mm in diameter followed by 25 mL of aqueous solution that was carefully poured or pipetted over the CCl<sub>4</sub>. The plate was lowered to a consistent depth, and the surface pressure was recorded after the interface came to equilibrium. For the air/water measurements, 25 mL solutions were prepared in crystallization dishes, covered, and allowed to stand 18 h to come to equilibrium. To make a measurement, the plate was lowered until it just touched the surface, and the surface pressure was recorded.

**C. Sum Frequency at a Liquid/Liquid Interface.** The 1064 nm output (with a top hat profile) of a Nd:YAG laser operating at 20 Hz with 3.5 ns pulse duration is split into two beams. The first is used to generate visible light at 532 nm by passing the fundamental through a doubling crystal with the power in the beam maintained at 5 mJ/pulse. The tunable IR (1900–4000 cm<sup>-1</sup>) is obtained by pumping an OPO—OPA with the other fundamental beam and provides 1–4 mJ/pulse with a bandwidth of 1 cm<sup>-1</sup>. The OPO employs a pair of KTP crystals that are angle tuned and configured to eliminate beam walk off. The OPA employs a pair of KTA crystals in the same manner. The IR is focused at the interface and overlapped in space and time with the 1 mm diameter visible beam. The input and output polarizations are controlled, and the sum frequency beam is collected with a PMT and gated electronics. The experiment is conducted in a total internal reflection (TIR) geometry which increases the sum frequency signal by more than 2 orders of magnitude.<sup>16,20–25</sup> Custom Teflon cells with CaF<sub>2</sub> windows served as the sample holders and allowed the TIR geometry. Fresh aqueous solution and CCl<sub>4</sub> were used for each interface examined. Time was allowed for equilibration of the interface.

**D. Sum-Frequency at an Air/Liquid Interface.** The laser system used in these experiments has been described previously.<sup>26,27</sup> The following is an overview of that system including some recent changes. A diode-pumped, frequency-doubled Nd:YVO<sub>4</sub> laser pumps a Ti:sapphire oscillator to produce 800 nm light in 140 fs pulses at 1 kHz. The pulses are stretched to 220 ps, amplified first in a regenerative amplifier and again in a double pass Ti:sapphire oscillator (both pumped by a Nd:YLF laser), and then compressed to 1.9 ps with a bandwidth of 18 cm<sup>-1</sup>. The resulting 2-W beam is split into four parts. Approximately 270 mW reaches the interface to provide the fixed frequency visible beam. Approximately 370 mW pumps an OPG (double pass through a magnesium-doped LiNbO<sub>3</sub> crystal) to produce a range of wavelengths which is dependent on the angle of the crystal. A grating selects the appropriate wavelength (around 1 μm) from this

light and directs it as the seed through a two-stage angle tuned OPA (each pumped by a portion of the 800 nm). The first stage relies on difference frequency mixing of the seed with 450 mW of the 800 nm in a KTA crystal to provide the tunable IR (2.4–4.0 μm). The second stage amplifies the IR in another KTA crystal pumped with 450 mW of the 800 nm. There is control over the input and output polarizations. The SF beam is collected with a thermoelectrically cooled CCD camera. The experiment is conducted in external reflection. Solutions were prepared using the same procedure as for surface tension, and the crystallization dishes served as the sample cells for the spectroscopy.

## 4. Results and Discussion

**A. Surface Tension.** It is important in the evaluation of the VSFS data to know the number density of molecules at the interface for each aqueous concentration of surfactant. Surface tension experiments are a standard method of determining the number of surface-active molecules at a liquid interface. After fitting the surface tension data to the Gibbs equation (eq 1), one can determine the surface concentration for any bulk concentration using the Frumkin equation (eq 2) and the known bulk concentration. Figure 2a–c shows the isotherms for DBS at the air/water interface, the air/water interface in the presence of excess salt, and the CCl<sub>4</sub>/water interface with excess salt. The CCl<sub>4</sub>/water interface in the absence of salt was not studied because reproducible isotherms could not be obtained. Every system studied here attained maximum surface coverage at aqueous bulk concentrations that fall below the cmc (9.8 mM for LDS and 1.2 mM for DBS<sup>28</sup>). The isotherm for LDS at the air/water interface in the absence of excess salt is shown in Figure 2d. The isotherm is steepest for DBS at the CCl<sub>4</sub>/water interface (Figure 2c) reaching a maximum surface pressure of 37 mN/m at a bulk concentration of ~40 μM. This is indicative of the highly absorptive nature of DBS at the CCl<sub>4</sub>/water interface. DBS adsorbs to a somewhat lesser degree at the air/water interface with excess salt with a maximum surface pressure of 40 mN/m at ~80 μM (Figure 2b). A lower surface activity is seen for DBS at the air/water interface (without excess salt) where the isotherm shows a more gradual rise with a maximum surface pressure of 42 mN/m at ~400 μM (Figure 2a). LDS at the air/water interface shows a much lower level of surface activity relative to DBS. The maximum surface pressure is attained beyond 3.5 mM (Figure 2d).

The limiting area per molecule at monolayer coverage can be determined by recasting the surface pressure data in the form of the Gibbs equation (pressure vs natural log of the concentration) and fitting the linear portion of the data. For DBS, the limiting area per molecule at the air/water interface in the absence of excess salt is 59 ± 3 Å<sup>2</sup> (1.7 × 10<sup>14</sup> molecules/cm<sup>2</sup>); in the presence of excess salt it is 47 ± 3 Å<sup>2</sup> (2.1 × 10<sup>14</sup> molecules/cm<sup>2</sup>). The limiting area for DBS at the CCl<sub>4</sub>/water interface in the presence of excess salt is 60 ± 3 Å<sup>2</sup> (1.7 × 10<sup>14</sup> molecules/cm<sup>2</sup>). For LDS the limiting area per molecule at the air/water interface in the absence of excess salt is 59 ± 3 Å<sup>2</sup> (1.7 × 10<sup>14</sup> molecules/cm<sup>2</sup>). The limiting area for LDS at the CCl<sub>4</sub>/water interface is (from previous work) 61 ± 4 Å<sup>2</sup> (1.6 × 10<sup>14</sup> molecules/cm<sup>2</sup>).<sup>29</sup> It is interesting that the area per molecule is the same for LDS and DBS at the air/water interface without excess salt considering the bulky headgroup on DBS. This result is suggestive of a staggered arrangement of the DBS headgroups at the interface. This is a reasonable picture in light

(18) Ramé, E. *J. Colloid Interface Sci.* **1997**, *185*, 245–251.

(19) Davies, J. T.; Rideal, E. K. *Interfacial Phenomena*; Academic Press: New York, 1961.

(20) Conboy, J. C.; Daschbach, J. L.; Richmond, G. L. *J. Phys. Chem.* **1994**, *98*, 9688–9692.

(21) Guyot-Sionnest, P.; Shen, Y. R.; Heinz, T. F. *Appl. Phys. B* **1987**, *42*, 237–238.

(22) Hatch, S. R.; Polizzotti, R. S.; Dougal, S.; Rabinowitz, P. *J. Vac. Sci. Technol.* **1993**, *11*, 2232–2238.

(23) Bloembergen, N.; Pershan, P. S. *Phys. Rev.* **1962**, *128*, 606–622.

(24) Bloembergen, N. *Opt. Acta* **1966**, *13*, 311–322.

(25) Bloembergen, N.; Simmon, H. J.; Lee, C. H. *Phys. Rev.* **1969**, *181*, 1261–1271.

(26) Gragson, D. E.; Alavi, D. S.; Richmond, G. L. *Opt. Lett.* **1995**, *20*, 1991–1993.

(27) Gragson, D. E.; McCarty, B. M.; Richmond, G. L.; Alavi, D. S. *J. Opt. Soc. Am. B* **1996**, *13*, 2075–2083.

(28) Mukerjee, P.; Mysels, K. J. *Critical Micelle Concentrations of Aqueous Surfactant Systems*; National Bureau of Standards: Washington, DC, 1971.

(29) Conboy, J. C.; Messmer, M. C.; Richmond, G. L. *Langmuir* **1998**, *14*, 6722–6727.



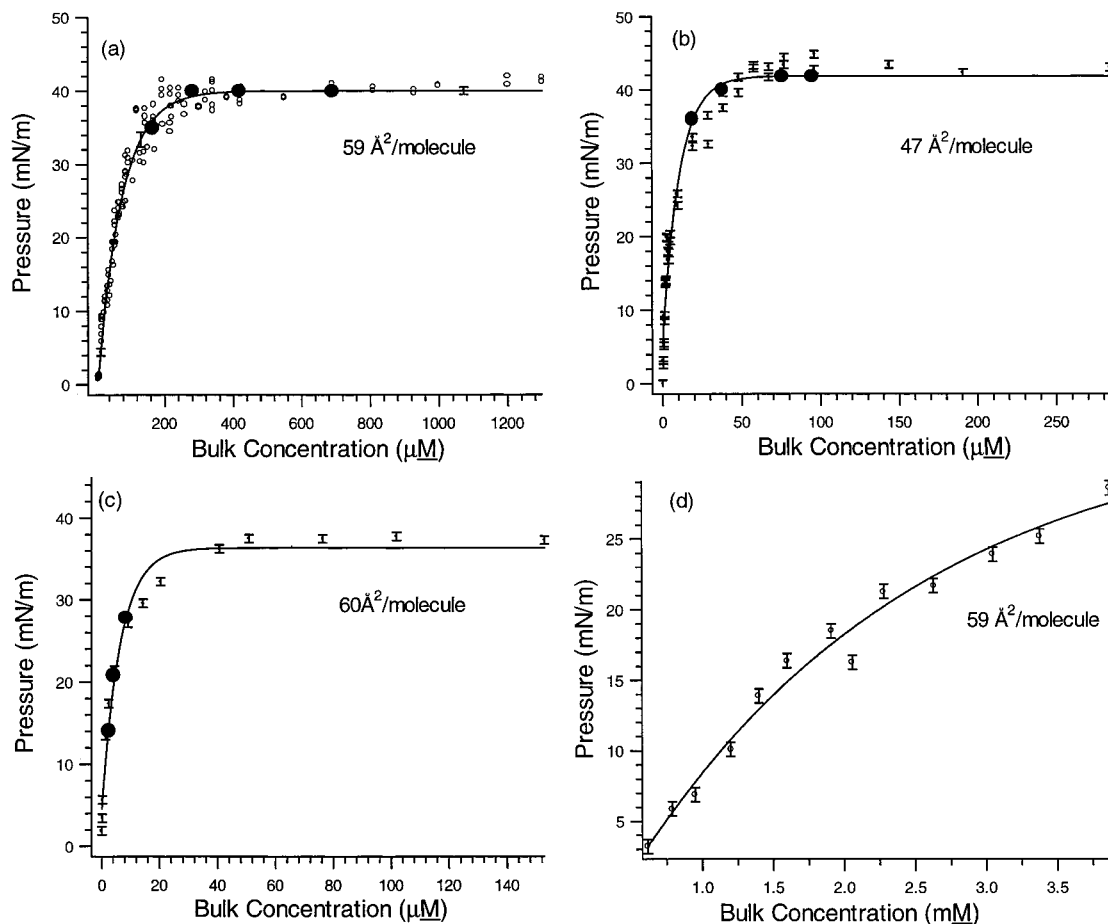


**Figure 2.** Surface pressure isotherms for (a) DBS at the air/water interface, (b) DBS at the air/water interface with 0.1 M NaCl, (c) DBS at the  $\text{CCl}_4$ /water interface with 0.1 M NaCl, and (d) LDS at the air/water interface. The solid points in (a)–(c) are concentrations and surface pressures corresponding to the solid data points in Figure 6a–c, respectively. The solid lines are fits to the Gibbs isotherm.

of the fluid nature of the interface. These ideas will be explored more fully later in the paper.

There are three parameters to be discussed in analyzing the macroscopic behavior of these surfactants at the liquid interface: the surface activity of the surfactant; the effect of excess salt; the presence of the adjacent nonaqueous phase. Here we use the constancy of the surface pressure with increased surfactant concentration as an indicator of monolayer formation. A comparison of LDS and DBS at the air/water interface shows that DBS is more surface active achieving monolayer formation at about 0.2 mM concentration in the aqueous phase whereas LDS reaches monolayer formation at several millimolar similar to other simple surfactants such as SDS and dodecyltrimethylammonium chloride.<sup>30</sup> We can attribute some of this difference to the larger hydrophobic group of the DBS. In general, increasing the size of the hydrophobic group of a surfactant results in monolayer formation at lower bulk concentration.<sup>11</sup> For example, the addition of two methylene units to an alkyl chain often results in reaching monolayer formation at 25–30% of the bulk concentration required for the shorter chain. A benzene ring is generally considered equivalent to 2–3 methylene units. Therefore, if the benzene ring is only adding length to the hydrophobic chain, one would not expect to see monolayer formation by DBS at ~5% of the bulk concentration required for LDS. We conclude that the ring plays a role in enhancing the surface activity. The polarizability of the conjugated headgroup which results in the large solubility of DBS in water

(orders of magnitude greater than LDS by concentration) probably contributes to the greater surface activity because the polarization of the headgroup can change to accommodate the polarity of the interface. Interestingly, despite the increased surface activity of DBS and the bulkier nature of the benzene ring, the actual density of molecules at full monolayer coverage is approximately the same for the two molecules.

For the air/water studies, addition of excess salt to the DBS reduces the area per molecule at monolayer coverage from 59 to 47  $\text{\AA}^2$ . We interpret this higher degree of packing at the interface to be due to screening of the charged sulfonate headgroups by sodium ions reducing the Coulombic repulsion between headgroups. The bulk concentration at which monolayer formation is complete also decreases, from ~200 to ~50  $\mu\text{M}$ . We attribute this to the excess sodium facilitating the adsorption of DBS at the interface as repulsion between headgroups is reduced. This effect has been documented for many soluble surfactants in previous studies.<sup>31</sup> The enhanced adsorption shifts the equilibrium of the adsorption/desorption process toward increased adsorption at lower bulk concentrations.

When the hydrophobic phase is changed from air to  $\text{CCl}_4$ , there is a further reduction in the bulk concentration required to achieve monolayer coverage from ~50 to ~20  $\mu\text{M}$  indicating a higher degree of surface activity for DBS at this liquid/liquid interface. However, at monolayer coverage the area per molecule is higher at the  $\text{CCl}_4$ /water interface, a value of 60  $\text{\AA}^2$ . We

(30) Conboy, J. C.; Messmer, M. C.; Richmond, G. L. *J. Phys. Chem. B* 1997, 101, 6724–6733.

(31) Durham, K. *Properties of Detergent Solutions-Amphipathy and Adsorption*; Durham, K., Ed.; Macmillan and Co. Limited: London, 1961; pp 1–28.

attribute both effects to solvation of the chains by  $\text{CCl}_4$  which shifts the adsorption equilibrium further in favor of adsorption at lower bulk concentrations due to the favorable energy of solvation of the chains ( $\Delta H_{\text{soln}} \sim 4.5$  kJ/mol per  $\text{CH}_2$  unit).<sup>32</sup> With the chains solvated, more space between molecules is necessary to accommodate the solvent.

**B. Spectroscopic Studies.** The VSFS spectra of DBS were obtained for the interfaces described in the previous section. All spectra were acquired using linearly polarized visible and IR light and by collecting linearly polarized light. The designations of *p* and *s* are used to describe light polarized in the plane of incidence and normal to the plane of incidence, respectively. In the experimental geometries employed in these studies, *p*-polarized light is polarized normal to the interface and *s*-polarized light is polarized in the plane of the interface. All polarization schemes are given in the format: sum frequency; visible; infrared. The spectra were fit with a multiple peak fitting routine (Igor Pro) utilizing a Voigt functional form for each peak. We chose the Voigt profile because the laser has a Gaussian frequency profile and the molecular vibrations have a Lorentzian profile. We begin the analysis with an assignment of vibrational modes to various spectral features followed by a discussion of spectral changes with concentration.  $\text{D}_2\text{O}$  was used in all the spectroscopic work instead of  $\text{H}_2\text{O}$  because the O–H stretch modes overlap with the C–H stretch modes of interest.

**Peak Assignments.** Figure 3 shows the VSFS spectra for DBS at the  $\text{CCl}_4/\text{D}_2\text{O}$  (Figure 3a,b) and air/ $\text{D}_2\text{O}$  (Figure 3c) interfaces. The spectra in Figure 3a,c show the entire C–H stretch region under *ssp* polarization, and Figure 3b shows the aromatic C–H stretch region under *sps* polarization at two different concentrations. All of the air/ $\text{D}_2\text{O}$  and the  $\text{CCl}_4/\text{D}_2\text{O}$  SF spectra share the same assignments. The C–H stretches of the alkyl chains under *ssp* polarization have been previously assigned for alkyl surfactants.<sup>33–35</sup> Since we do not expect any significant frequency shifts in these modes with the addition of the aromatic moiety, similar assignments are made here. The peaks at 2850, 2874, 2930, and 2917  $\text{cm}^{-1}$  are assigned to the methylene symmetric stretch ( $\text{CH}_2\text{SS}$ ), the methyl symmetric stretch ( $\text{CH}_3\text{SS}$ ), the methylene asymmetric stretch ( $\text{CH}_2\text{AS}$ ), and the methylene Fermi resonance (FR), respectively.

The peaks between 3000 and 3100  $\text{cm}^{-1}$  belong to aromatic C–H stretching modes and are assigned by comparison to the IR and Raman assignments for similar compounds compiled by Varsanyi<sup>36</sup> and Bain et al.<sup>37,38</sup> The C–H stretching modes of benzene in this region are  $\nu_2$ ,  $\nu_{7a}$ ,  $\nu_{7b}$ ,  $\nu_{20a}$ , and  $\nu_{20b}$ .<sup>36</sup> Since DBS is of  $C_s$  symmetry, all vibrational modes are IR and Raman active and are therefore sum-frequency allowed. Thus none of these modes can be dismissed due to the symmetry requirements of VSFG. However, we can dismiss mode 7a because it drops to a few hundred wavenumbers in energy for a para-substituted benzene (like DBS) where one substituent has a light atom bonded to the ring and the other has a heavy atom bonded to the ring.<sup>36</sup> The other modes appear in the following order by

(32) Fuchs, R.; Chambers, E. J.; Stephenson, W. K. *Can. J. Chem.* **1987**, *65*, 2624–2627.

(33) Conboy, J. C.; Messmer, M. C.; Richmond, G. L. *J. Phys. Chem.* **1996**, *100*, 7617–7622.

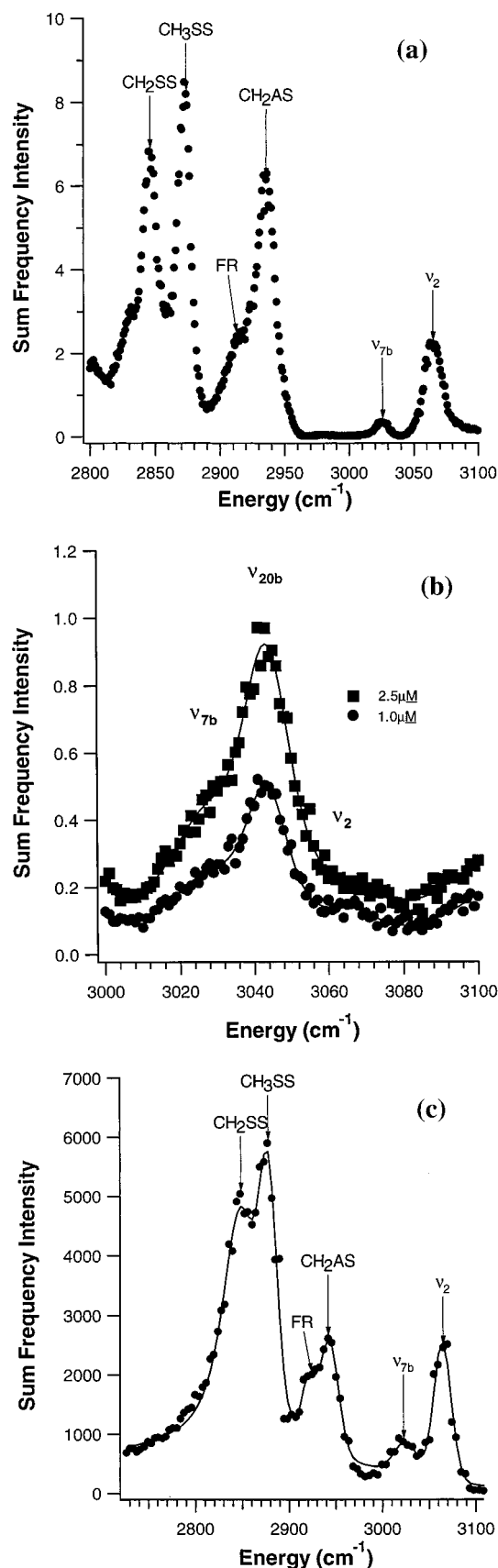
(34) MacPhail, R. A.; Strauss, H. L.; Snyder, R. G.; Elliger, C. A. *J. Phys. Chem.* **1984**, *88*, 334–341.

(35) Snyder, R. G.; Strauss, H. L.; Elliger, C. A. *J. Phys. Chem.* **1982**, *86*, 5145–5150.

(36) Varsanyi, G. *Assignments for Vibrational Spectra of Seven Hundred Benzene Derivatives*; John Wiley & Sons: New York, 1974; Vol. 1.

(37) Bain, C. D.; Li, Z. X.; Bell, G. R. *J. Phys. Chem. B* **1998**, *102*, 9461–9472.

(38) Bain, C. D.; Bell, G. R.; Duffey, D. C.; Ward, R. N. *Mol. Phys.* **1996**, *88*, 269–280.

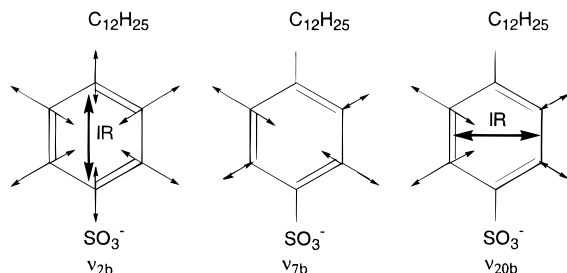
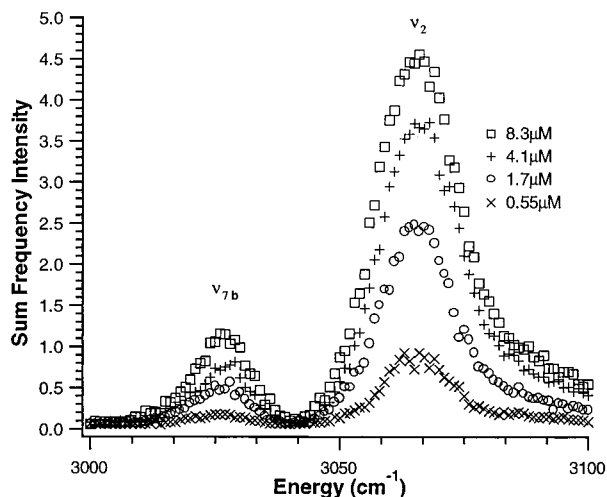


**Figure 3.** VSFS of (a) DBS at the  $\text{CCl}_4/\text{D}_2\text{O}$  interface, 0.1 M NaCl, *ssp* polarization, (b) DBS at the  $\text{CCl}_4/\text{D}_2\text{O}$  interface, 0.1 M NaCl, *sps* polarization, and (c) DBS at the air/ $\text{D}_2\text{O}$  interface, 0.1 M NaCl, *ssp* polarization. Solid lines are fits to the data assuming a Voigt functional form for the peaks.

**Table 1.** Vibrational Assignments for VSFS Peak Frequencies ( $\text{cm}^{-1}$ ) in the Aromatic C–H Stretch Region ( $3000\text{--}3100\text{ cm}^{-1}$ )

VSFS peak posns <sup>a</sup>	vibrational mode <sup>b</sup>	Varsanyi's peak posns
3029	$\nu_{7b}$	$3030 \pm 10$
3042	$\nu_{20b}$	$3040 \pm 10$
3065	$\nu_2$	$3060 \pm 10$
	$\nu_{20a}$	$3085 \pm 5$

<sup>a</sup> All positions  $\pm 2\text{ cm}^{-1}$ . <sup>b</sup> The modes always appear in this order of ascending energy.

**Figure 4.** Normal aromatic C–H stretch modes of DBS.**Figure 5.** VSFS of the aromatic C–H stretch region for a range of bulk concentrations of DBS at the  $\text{CCl}_4/\text{D}_2\text{O}$  interface, 0.1 M NaCl, and *ssp* polarization.

energy  $\nu_{7b}$ ,  $\nu_{20b}$ ,  $\nu_2$ , and  $\nu_{20a}$  at  $\sim 3030$ ,  $\sim 3040$ ,  $\sim 3060$ , and  $\sim 3080\text{ cm}^{-1}$ , respectively, with  $\nu_{20a}$  generally very weak or unobserved. On the basis of the similarities in frequency, we make the spectral assignments as shown in Table 1. Figure 4 shows the normal modes,  $\nu_2$ ,  $\nu_{7b}$ , and  $\nu_{20b}$ , of DBS.

**Aromatic Ring Orientation.** We examined the changes in the integrated intensity of the C–H stretching modes of the aromatic ring of DBS as a means of monitoring changes in the orientation of the headgroup in DBS as a function of increasing surface concentration.  $\nu_2$  was chosen as the mode to study because it is the most intense, and it is well resolved. For rings oriented perpendicular to the interface the transition moment for  $\nu_2$  lies along the surface normal and can be accessed with the *ssp* polarization scheme. Figure 5 shows representative *ssp* spectra spanning the aromatic C–H stretch region of DBS at the  $\text{CCl}_4/\text{D}_2\text{O}$  interface with excess salt for several concentrations of DBS. Both modes ( $\nu_{7b}$  at  $3029\text{ cm}^{-1}$  and  $\nu_2$  at  $3065\text{ cm}^{-1}$ ) increase monotonically in intensity with increasing surface concentration. Since the sum-frequency intensity depends on both the square of the number density and the orientational average of the molecules, a plot of the square root of the SF intensity against the number density of surfactant

molecules at the interface will be linear if the average orientation of the surfactant headgroup is not changing and curved if the average orientation is changing as a function of concentration. Figure 6a–c shows these plots for the following interfaces respectively: air/ $\text{D}_2\text{O}$ ; air/ $\text{D}_2\text{O}$  with excess salt;  $\text{CCl}_4/\text{D}_2\text{O}$  with excess salt. Each series of measurements spans the rising portion of the surface pressure isotherm up to monolayer surface coverage.

Figure 6a indicates that for the air/ $\text{D}_2\text{O}$  interface the SF intensity in the  $\nu_2$  mode is relatively constant up to approximately  $1.4 \times 10^{14}$  molecules/ $\text{cm}^2$  after which there is a sharp rise with interfacial DBS concentration. For clarity, solid points represent data collected near monolayer formation as indicated by surface tension data. These points correspond to the solid points on the isotherm in Figure 2a. The sharp rise in SF intensity as monolayer coverage is approached suggests that the average orientation of the aromatic rings changes significantly at the air/ $\text{D}_2\text{O}$  interface as monolayer coverage occurs. This increase in intensity suggests that the rings are becoming increasingly oriented perpendicular to the interface since we are probing vibrational modes normal to the interface. This same trend is observed at the air/ $\text{D}_2\text{O}$  interface for DBS in 0.1 M NaCl solution (Figure 6b) although the rise in intensity occurs at a higher surface density (than in the salt free solutions) corresponding to the plateau of the surface pressure isotherm (Figure 2b). We attribute this reorientation at the higher coverages to increased interaction between benzene rings of adjacent surfactant molecules and/or congestion due to the bulky nature of the headgroup.

For the  $\text{CCl}_4/\text{D}_2\text{O}$  interface with 0.1 M NaCl a very different behavior is observed for the orientation of the aromatic moiety. Figure 6c shows a nearly linear dependence of the square root of the sum-frequency intensity on surface number density as the interface approaches monolayer coverage. (As described previously, the solid data points correspond to the solid data points on the isotherm in Figure 2c.) This trend suggests that at the  $\text{CCl}_4/\text{D}_2\text{O}$  interface the rings do not change their average orientation with coverage. In this case, the dependence of the sum-frequency field can be directly related to a single factor: the number density of DBS molecules at the interface.

More information can be obtained about the orientation of the aromatic rings by examining spectra collected with the *ssp* and *sps* polarization schemes, and the result of this analysis is consistent with the lack of reorientation of the rings described above at the  $\text{CCl}_4/\text{D}_2\text{O}$  interface (Figure 6c). In Figure 3a is a representative *ssp* spectrum that clearly shows two modes:  $\nu_2$  and  $\nu_{7b}$  at  $3065$  and  $3029\text{ cm}^{-1}$ , respectively. For *sps* spectra (represented in Figure 3b) two modes are apparent,  $\nu_{7b}$  and  $\nu_{20b}$  at  $3029$  and  $3042\text{ cm}^{-1}$ , respectively, with a third weaker mode at  $3065\text{ cm}^{-1}$  which we assign to  $\nu_2$ . The transition dipole for  $\nu_2$  lies vertically (along the line connecting the substituents) in the plane of the ring (Figure 4). This mode is very strong in the *ssp* spectrum which detects modes aligned normal to the interface and very weak in the *sps* spectrum which detects modes aligned in the plane of the interface. This behavior is observed at all interfacial concentrations and indicates that the ring is oriented nearly vertical to the interface at all interfacial concentrations. A similar analysis of  $\nu_{20b}$  supports this conclusion. The transition dipole for  $\nu_{20b}$  lies horizontally (perpendicular to the line connecting the substituents) in the plane of the ring. This mode is strong in the *sps* spectrum and undetected in the *ssp* spectrum. The transition dipole for  $\nu_{7b}$  lies off axis, and there is appreciable intensity in both the *ssp* and *sps* spectra so we conclude that the ring is oriented near vertical at the

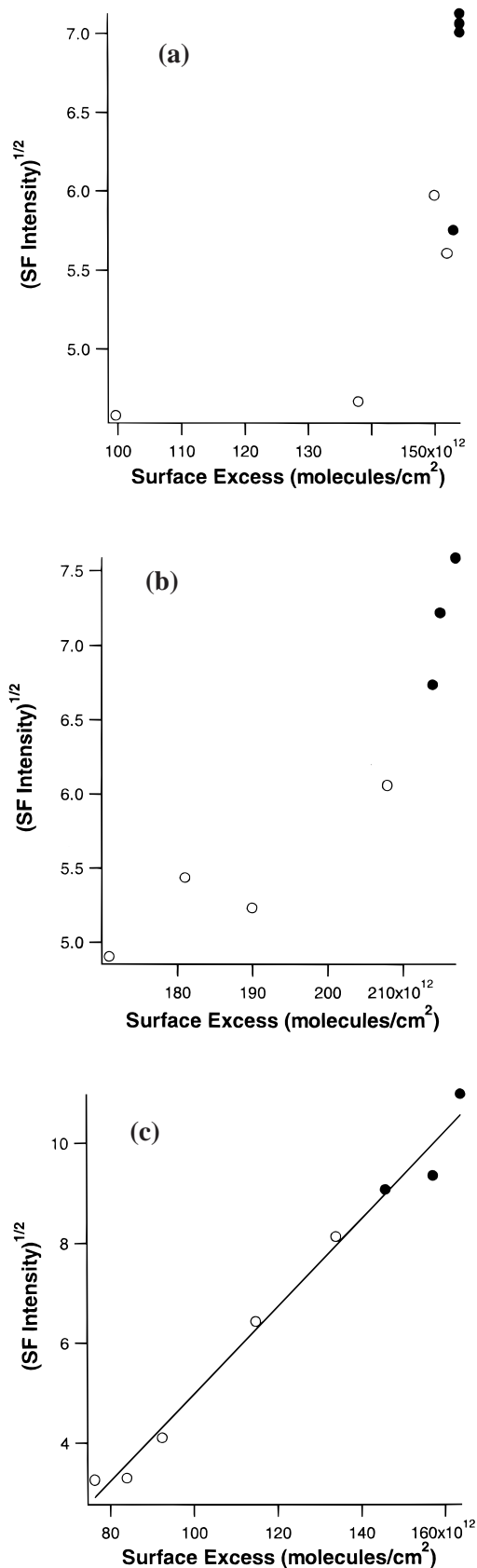


**Figure 6.** Square root of sum-frequency intensity of the mode  $\nu_2$  as a function of surface concentration for (a) DBS at the air/water interface, (b) DBS at the air/water interface with 0.1 M NaCl, and (c) DBS at the  $\text{CCl}_4/\text{water}$  interface with 0.1 M NaCl. (The line is a fit to the data.) The solid data points in (a)–(c) correspond to the concentrations and surface pressures indicated by the solid points in Figure 2a–c, respectively.

interface throughout the concentration range studied. We attribute the initial and continued orientation of the benzene ring of DBS to several factors including the highly aligned nature of water molecules in the  $\text{CCl}_4/\text{water}$  interfacial region<sup>39</sup> and the solvation of the aromatic/sulfonate headgroup region by solvent molecules in the interfacial region. This will be discussed further in more detail below. It would be interesting to compare these DBS results with similar ring orientation studies at the air/water interface, but we have not been able to obtain *sps* spectra of the aromatic C–H stretch region of DBS at the air/water interface due to low signal levels.

**Chain Conformation.** One of the objectives of this study was to determine what influence, if any, the aromatic ring has on the conformation of the alkyl chain at either or both of the liquid interfaces. The ratio of the integrated methyl symmetric stretch intensity to the integrated methylene symmetric stretch intensity is a useful parameter for examining the relative ordering of the alkyl chains at the interface.<sup>35</sup> For *p*-polarized IR, an all-trans chain results in the transition moment for the methyl symmetric stretch aligned in the direction of the electric field to produce a large SF signal. However, since there are local inversion centers at the center of each C–C bond in an all-trans alkyl chain, intensity in the methylene symmetric stretch band is SF forbidden under the dipole approximation (the Raman and IR moments are  $180^\circ$  out of phase). Conversely, under this same polarization (*ssp*), highly disordered chains result in an isotropic orientation of the methyl groups (producing much less SF intensity), and the gauche defects in the alkyl chains result in increased intensity in the methylene symmetric stretch. Thus, for perfect order the intensity ratio,  $\text{CH}_3\text{SS}/\text{CH}_2\text{SS}$ , approaches infinity with the methylene symmetric stretch absent and the methyl symmetric stretch strong. A much smaller ratio is expected with increased disorder as the methylene mode becomes dominant over the methyl mode. Representative ratios measured in this laboratory for some common molecules at monolayer coverage include 2.8 for dilauroylphosphocholine,<sup>40</sup> 2.4 for *n*-dodecylammonium chloride, and 1.4 for SDS<sup>30</sup> at the  $\text{CCl}_4/\text{D}_2\text{O}$  interface. Under *ssp* polarization there is intensity in both the  $\text{CH}_3\text{SS}$  and  $\text{CH}_2\text{SS}$  modes. Under *sps* polarization the  $\text{CH}_3\text{SS}$  intensity is low and difficult to resolve from other spectral features resulting in uncertain fitting of the peak. For these reasons the analysis of chain conformation will be confined to *ssp* spectra.

Figure 7 shows the dependence of the methyl-to-methylene ratio on surface concentration for (a) LDS at the air/water interface, (b) DBS at the air/water interface, (c) DBS at the air/water interface with 0.1 M NaCl, and (d) DBS at the  $\text{CCl}_4/\text{water}$  interface with 0.1 M NaCl. The data for LDS at the air/ $\text{D}_2\text{O}$  interface (Figure 7a) show an increase in the ratio with interfacial concentration, reaching a maximum coincident with maximum interfacial concentration as indicated by surface tension data (Figure 2d). In this respect LDS behaves like many common simple surfactants such as SDS and dodecyltrimethylammonium chloride:<sup>30</sup> the order of the chains increases as the surface concentration increases. This effect has been attributed to van der Waals forces between the chains.<sup>11,41,42</sup>

In stark contrast to this behavior is that of DBS at the air/ $\text{D}_2\text{O}$  interface (Figure 7b). The figure shows that the ratio is

(39) Chang, T. M.; Dang, L. X. *J. Chem. Phys.* **1996**, *104*, 6772–6783.

(40) Walker, R. A.; Conboy, J. C.; Richmond, G. L. *Langmuir* **1997**, *13*, 3070–3073.

(41) MacRitchie, F. *Chemistry at Interfaces*; Academic Press: San Diego, CA, 1990.

(42) Tanford, C. *The Hydrophobic Effect: Formation of Micelles and Biological Membranes*; John Wiley & Sons: New York, 1973.



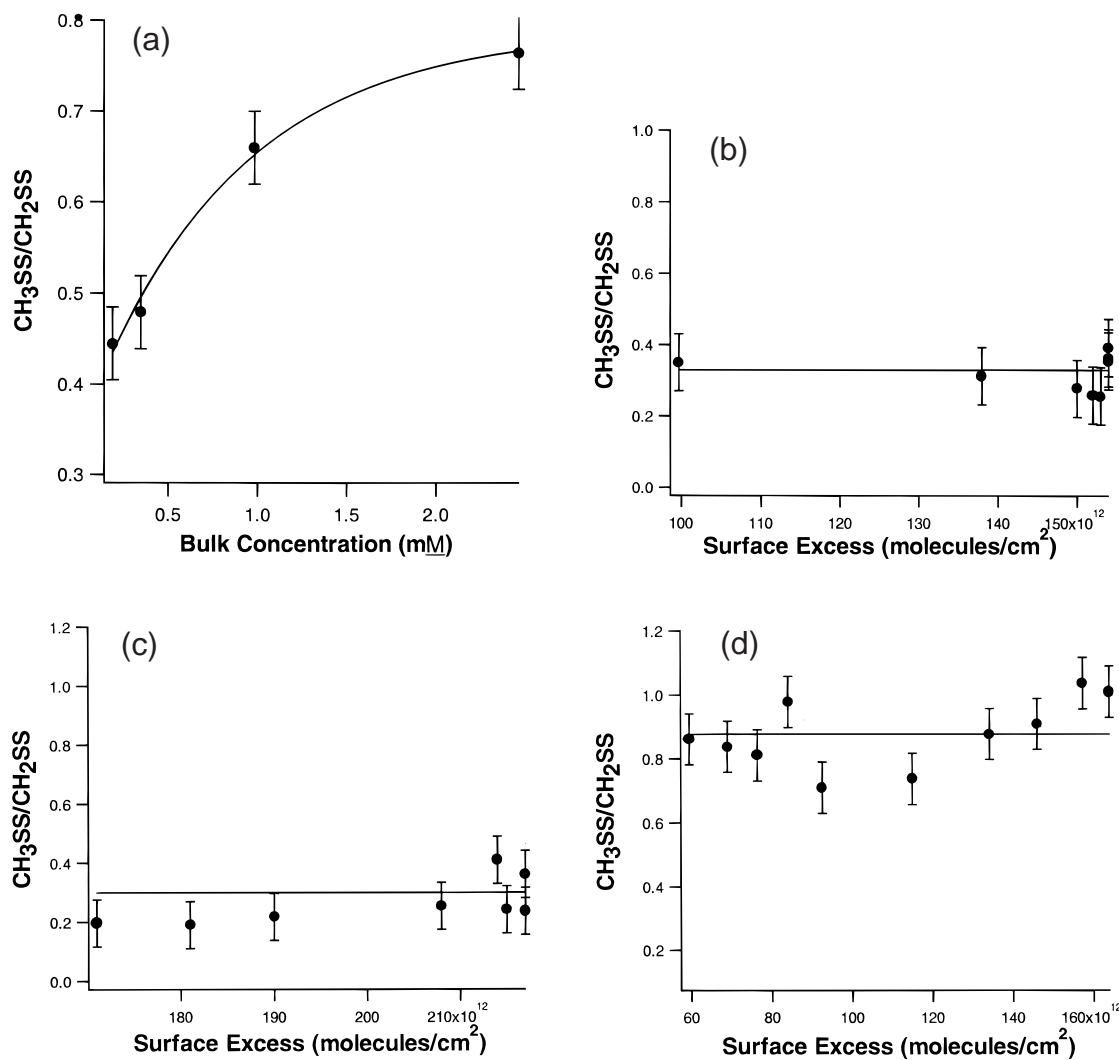


**Figure 7.** Ratio of the methyl to methylene symmetric stretch intensities as a function of surface concentration for (a) LDS at the air/water interface, (b) DBS at the air/water interface, (c) DBS at the air/water interface with 0.1 M NaCl, and (d) DBS at the  $\text{CCl}_4$ /water interface with 0.1 M NaCl. (The analogous data for LDS can be found in ref 28.) Each data point represents the average obtained from three spectra, and the error bars cover one standard deviation. (Lines are provided as a guide to the eye.)

relatively low ( $\sim 0.4$ ) and is essentially constant across the concentration range up to and beyond monolayer coverage. This indicates that there is essentially no change in the ordering of the chains in this system as the interfacial concentration increases. The chains are disordered at low surface concentrations and remain that way up to monolayer coverage. The addition of salt to the system allows the DBS molecules to get closer together as evidenced in the surface tension measurements (Figure 2b) with the area per molecule at monolayer coverage decreasing from 59 to 47  $\text{\AA}^2$ . One might expect this tighter packing to lead to greater interactions between the chains and increased order. However, with excess salt (Figure 7c) the ratio is also low and remains essentially constant up to and beyond monolayer coverage indicating that there is no appreciable change in the chain ordering.

With the change of the hydrophobic phase from air to  $\text{CCl}_4$  the chain behavior remains the same. Figure 7d shows that the ratio is essentially constant for DBS at the  $\text{CCl}_4/\text{D}_2\text{O}$  interface again indicating that the average chain conformation does not depend on surface concentration. Just as the chain conformation dependence on surface concentration is quite different for DBS and LDS at the air/ $\text{D}_2\text{O}$  interface so too is it quite different at the  $\text{CCl}_4/\text{D}_2\text{O}$  interface. Previous work in this laboratory has shown that the ordering of the LDS chains at the  $\text{CCl}_4/\text{D}_2\text{O}$

interface changes significantly with increasing surface concentration (from a low of 0.5 to a maximum of 1.3 at monolayer coverage) with the chains becoming more ordered with surface concentration<sup>29</sup> similar to what is observed here for LDS at the air/water interface.

In all three DBS systems studied, there is essentially no change in the degree of alkyl chain ordering with concentration, although the position of gauche defects (absolute conformation) in the chain may be changing. The low  $\text{CH}_3\text{SS}$  intensity in the *sps* spectra compared to that in the *ssp* spectra is evidence for the time-averaged alignment of the methyl group to be primarily along the interface normal. One might conclude that the low  $\text{CH}_3\text{SS}$  intensity in the *sps* spectra is a result of a center of symmetry in the plane of the interface; however, SFG is not symmetry forbidden in this case. As long as there is a lack of inversion symmetry in three dimensions, SFG can occur. The absence of methyl asymmetric stretch intensity at  $\sim 2960\text{ cm}^{-1}$  in the *ssp* spectra (Figure 3a,c) and its presence in the *sps* spectrum ( $\text{CCl}_4/\text{D}_2\text{O}$ ) supports this orientation of the methyl groups because the transition dipole for the asymmetric stretch is perpendicular to that of the symmetric stretch.

Comparison of the DBS and the LDS data shows that the presence of the benzene ring has a significant influence on chain



disorder for DBS relative to LDS. If the benzene rings were present at the interface in a horizontal plane such as might be expected for their adsorption on a solid surface, one would anticipate that the bulky nature of the benzene ring would reduce the ability for the first few adjacent methylene units to interact (by van der Waals interactions) with those on neighboring DBS molecules. However, the similar surface limiting areas for LDS and DBS suggest instead that the headgroup/benzene region of the DBS molecules arrange in more of a staggered configuration at the liquid interface. In this picture the headgroups would penetrate to different degrees into the interfacial region. Such staggering of adjacent headgroups would reduce the interaction between the first few methylene groups of neighboring DBS molecules relative to LDS. The polarizable nature of the benzene ring of DBS should at some level facilitate this staggered arrangement relative to the less polarizable initial methylene units of LDS. The degree to which DBS headgroup region would be solvated by molecules in the  $\text{CCl}_4$ /water interface depends on the dimensions and composition of the interfacial region. Some insight into the properties and dimensions of the  $\text{CCl}_4$ /water interface have been provided by molecular dynamics calculations.<sup>39,43</sup> These studies indicate a roughness, or mixed-solvent interphase region, of approximately 7 Å thickness.

This idea that chain–ring interactions can alter the alkyl ordering at these liquid interfaces is also supported by chain length arguments. At an air/water interface, hydrocarbon chain order would be expected to increase with chain length as the opportunity for van der Waals interactions increases. If one were to view the effect of the benzene ring as simply an increase in hydrocarbon chain length, then one would expect to see greater alkyl chain ordering for DBS relative to LDS, contrary to what is observed. What is rather surprising is the fact that even at high interfacial DBS concentrations, there is no evidence for enhanced alkyl chain ordering by chain–chain interactions. This would suggest that the ordering in the first few methylene units and the dynamics of interface largely control alkyl chain conformations at these liquid interfaces.

At the air/water interface, interactions between the aromatic rings on DBS clearly affect the orientation of the rings as the surface concentration increases. This is evidenced by the observed change in ring orientation toward a vertical geometry as the surface concentration increases. This reorientation appears to have a negligible effect on alkyl chain ordering. At the  $\text{CCl}_4$ /water interface, the lack of ring reorientation with surface coverage suggests that the rings are initially aligned in an orientation perpendicular to the interface and that this does not change with interfacial concentration. A second possible explanation is that the interaction between adjacent benzene rings in the  $\text{CCl}_4$ / $\text{D}_2\text{O}$  interface is not as important as the interactions between the ring and the mixture of solvent molecules in the interfacial region. We believe that both effects are at play here. Calculations by Chang and Dang<sup>39</sup> indicate that there is an interfacial potential of several hundred millivolts at the  $\text{CCl}_4$ /water interface created by the orientation of water and  $\text{CCl}_4$  at this interface. Recent VSFS studies show a high degree of orientation of water at this neat interface.<sup>44</sup> For the air/DBS/water studies, the benzene rings do not show such a strong initial alignment but they do indicate that the presence of the polar water phase has less of an impact on screening adjacent benzene rings than is apparent for the liquid/liquid interface.

## 5. Conclusions

The enhanced efficacy of linear alkyl benzene sulfonates over linear alkanesulfonates has been known for many years. The experiments described herein were designed to investigate the molecular structure and interactions of these two types of surfactants at liquid/air and liquid/liquid ( $\text{CCl}_4$ / $\text{D}_2\text{O}$ ) interfaces. Although these studies were conducted on planar surfaces, insight derived from such model studies has relevance to surfactant interactions in surfactant assemblies such as micelles. This study provides some of the first molecular level measurements of how differently these surfactants behave at these two types of interfaces.

The most striking difference between the alkane- and alkylbenzenesulfonate surfactants is the conformation of their alkyl chains. At both interfaces, the VSFS measurements of the C–H stretching region show that the alkyl chains of LDS increase in conformational ordering as the interfacial concentration is increased. For DBS, a high degree of gauche defects in the chain is apparent at all concentrations relative to LDS. We attribute this difference in conformational ordering to the presence of the benzene ring in DBS. The limiting surface area measurements support a picture that DBS surfactants exist in a staggered headgroup geometry, a picture consistent with the benzene rings disrupting chain–chain interactions for the first few methylene groups adjacent to the benzene ring in DBS. This staggered arrangement appears to result in significantly disordered alkyl chains for DBS at both interfaces even though one might expect the strongest effect to be in only the first few methylene units of the surfactant. There is no evidence for DBS that increased surface concentration and subsequent packing of alkyl chains can overcome this disruption. This staggered geometry for DBS is most likely facilitated by the polarizable nature of the benzene ring.

This is the first VSFS study that has measured the three high-energy C–H stretching modes of an aromatic adsorbate at an interface and used the information to study the dependence of the orientation of the ring on interfacial concentration. In the liquid/liquid studies, the benzene rings appear oriented perpendicular to the interface and this orientation is not affected by changes in interfacial concentration even up to a monolayer. This is in stark contrast to what is observed at the air/water interface where increased orientation of the benzene ring in the perpendicular direction is observed as a monolayer of coverage is approached. We attribute this difference to a combination of factors including the staggering of adjacent benzenesulfonate headgroups in the interfacial region, alignment by the  $\text{CCl}_4$ / $\text{D}_2\text{O}$  interfacial potential, and the solvation of the benzene ring in the interphase  $\text{CCl}_4$ / $\text{D}_2\text{O}$  region.

The molecular properties that lead to the high solubility of DBS in water relative to LDS seem to also play a role in how these molecules adsorb at a hydrophobic/hydrophilic surface. If behavior similar to what we observe on a planar liquid surface is occurring as these surfactants form micelles, one has a picture of the DBS environment in the micelle as having a more fluidlike nature relative to LDS due to the disordering of the alkyl chains. Such observations and conclusions might be factors in the difference in efficacy of these two surfactants as detergents.

**Acknowledgment.** The authors gratefully acknowledge support from the Department of Energy, Basic Energy Sciences Grant DE-FG06-86ER45273, and the Petroleum Research Fund of the American Chemical Society.

(43) Michael, D.; Benjamin, I. *J. Chem. Phys.* **1997**, *107*, 5684–5693.

(44) Scatena, L.; Richmond, G. L. To be submitted for publication.